# A Molecular Communication Perspective on Detecting Arterial Plaque Formation

Pit Hofmann*, *Graduate Student Member, IEEE*, Sebastian Schmidt*, *Graduate Student Member, IEEE*, Alexander Wietfeld*, *Graduate Student Member, IEEE*, Pengjie Zhou, Jonas Fuchtmann, Frank H.P. Fitzek, *Senior Member, IEEE*, and Wolfgang Kellerer, *Senior Member, IEEE*

***Abstract*—The formation of plaques in human blood vessels, known as *atherosclerosis*, represents one of the major causes of death worldwide. Synthetic molecular communication (MC), in combination with nanotechnology, is envisioned to enable novel approaches toward diagnosing, monitoring, and treating diseases. In this paper, we propose an investigation of the effects of plaque formation on the human blood vessel as an MC channel. By characterizing these changes, the early detection of plaques using MC networks in the human circulatory system could become possible. We model a simplified blood flow scenario in a human carotid artery using OpenFOAM. Nanoparticles are released in the bloodstream in front of a region obstructed by a plaque, and their transport and distribution are evaluated as they pass through. The results are obtained for different plaque sizes and channel lengths. We observe a significant impact of a growing plaque on the channel characteristics in terms of a reduced propagation delay and a decrease in the cumulative number of received particles due to particles trapped by the plaque. Therefore, the receiver could detect abnormalities from a change in these channel conditions over time. Further investigation of these methods in conjunction with more realistic modeling of the channel and communication nodes will be necessary to confirm the results. It could contribute towards advanced future methods of diagnosis.**

***Index Terms*—Internet of Bio-Nano Things, microfluidic molecular communication, OpenFOAM, plaque formations, simulation**

## I. Introduction

THE convergence of nanotechnology and communication paradigms has paved the way for innovations in the field of bioengineering and healthcare. Among these innovations, molecular communication (MC) stands out as a promising paradigm for enabling communication at the nanoscale, facilitating the exchange of information among bio-nano machines (BNM) [1]. The emerging concept of the Internet of Bio-Nano Things (IoBNT) has gained attention, providing a networked ecosystem where BNM communicate to monitor and control various biological processes [1]. One intriguing application of the IoBNT could lie in addressing the issue of arterial plaque formation or *atherosclerosis*. This paper explores the interdisciplinary synergy in MC between biology, nanotechnology, and communications engineering, and their potential role in early plaque detection strategies to address this pervasive health challenge.

It is important to differentiate between natural and synthetic MC. Natural MC is often used to denote processes that are inherent to biological systems and their regulation mechanisms. *Synthetic* MC denotes separate or auxiliary communication processes that are artificially set up, for example, inside the human body to monitor, support, or repair natural functionality. In the envisioned scenario, a large number of BNM is deployed within the human cardiovascular system. The BNM communicate using nanoparticles or molecules, which are transported by diffusion and flow through the blood vessels. These BNM could serve as agents for fulfilling various tasks, such as detection, transport, or release of particles and molecules.

There has been extensive research from the perspective of modeling natural MC as a communication-theoretic process. In [2], detailed simulations are used to analyze the molecular interactions inside the blood vessel in the early stages of atherosclerosis, called *atherogenesis*. From the perspective of MC, *platelets* act as transmitters of a messenger protein towards the *endothelial cells*, which bind the protein at the walls of the blood vessel. Usually, this process is started to combat a blood vessel injury. However, in the case of anomalous behavior, the protein binding starts a kind of chain reaction that leads to the initial build-up of fatty tissue as a plaque at the arterial walls. In the paper, the process is modeled in detail, and the effect of various parameters on the delay and speed of the binding is investigated [2]. In a significant extension of the previous work, the authors additionally propose a mathematical Markov chain model and perform laboratory experiments to match the previous simulation of the natural MC system behind *atherogenesis* [3]. Research into MC models of in-body processes can support the development of diagnosis and treatment methods by providing a unique communication-theoretic perspective.

Alexander Wietfeld and Wolfgang Kellerer are with the Chair of Communication Networks, Technical University of Munich, Germany. Sebastian Schmidt was with the Chair of Communication Networks, Technical University of Munich, Germany, until March 2024. email: {alexander.wietfeld, sebastian.a.schmidt, wolfgang.kellerer}@tum.de.

Pit Hofmann, Pengjie Zhou, and Frank H.P. Fitzek are with the Deutsche Telekom Chair of Communication Networks, Technische Universität Dresden, Dresden, Germany; F. Fitzek is also with the Centre for Tactile Internet with Human-in-the-Loop (CeTI), Dresden, Germany, email: {pit.hofmann, pengjie.zhou, frank.fitzek}@tu-dresden.de.

Jonas Fuchtmann is with the Minimally Invasive Interdisciplinary Therapeutical Intervention (MITI), Klinikum rechts der Isar, Technical University Munich, Munich, Germany, email: jonas.fuchtmann@tum.de.

This work was supported by the German Research Foundation (DFG) as part of Germany's Excellence Strategy—EXC 2050/1—Cluster of Excellence "Centre for Tactile Internet with Human-in-the-Loop" (CeTI) of Technische Universität Dresden under project ID 390696704 and the Federal Ministry of Education and Research (BMBF) in the programme of "Souverän. Digital. Vernetzt." Joint project 6G-life, grant numbers 16KISK001K and 16KISK002. This work was also partly supported by the project IoBNT, funded by the German Federal Ministry of Education and Research (BMBF) under grant number 16KIS1994. *P. Hofmann, S. Schmidt, and A. Wietfeld contributed equally to this work and are listed as co-first authors in alphabetical order of the surnames.

In this paper, we take the opposite approach and attempt to use the properties of synthetic MC that is unrelated to any natural biological process to reveal potential in-body processes that affect the artificial communication channel. For this purpose, no deeper analysis of the underlying biological messaging is necessary. Specifically, we focus on combining ongoing synthetic MC research with the concept of sensing and detecting plaque formation using the example of the carotid artery. Therefore, we model the blood flow in a blood vessel using OpenFOAM, adding plaque of varying sizes, i.e., at different stages of growth. From an analytical point of view, we need accurate MC channel models for the design, analysis, and reliable operation of MC systems [4]. The state-of-the-art channel models for advection do not yet consider obstacles, for example, plaque formations, in the communication channel [4].

In [5], a number of different obstacles were placed in an experimental system and were found to not degrade or even improve communication performance. However, the investigated system was of a much larger scale than blood vessels. In [6], shapes were examined via simulations, specifically as decelerators in the flow channel, to reduce the dispersion of the MC pulse. The scale used is similar to blood vessels, and the obstacles are found to have both accelerating and decelerating effects. However, in this case, obstacles were deliberately designed to benefit communication. None of the papers interpreted the obstacles as a medical sensing issue. In contrast, we propose to use an undesirable and initially unknown change in channel conditions due to the narrowing channel and the change in flow speed in the plaque region as an indicator for detecting the plaque itself. This could be implemented via dedicated periodic pilot symbols sent by the BNM in the bloodstream or alternatively by interpreting the received signal from symbols sent for the purpose of unrelated MC between the BNM, for example, synchronization messages, resulting in a type of joint communication and sensing scheme.

## II. Medical Background

### A. Plaque Formation and Prevalence

The formation of plaque within human arteries, a process known as *atherosclerosis* [7], is a complex and multifaceted phenomenon with significant implications for human cardiovascular health. *Atherosclerosis* involves the gradual accumulation of lipids, inflammatory cells, and fibrous tissue within the arterial walls, leading to the development of *atherosclerotic* plaques. These plaques can compromise the blood flow, increasing the risk of ischemic events like strokes.

Several risk factors contribute to the development of plaque, including hypertension, hyperlipidemia, smoking, and diabetes. Therefore, *atherosclerosis* represents a significant health problem, being the most common cause of cardiac death and constituting about 30 % of all deaths worldwide [8]. Specifically, plaques in the carotid artery are estimated to affect about 21.1 % of the world's population between the ages of 30 and 79, with an increase in the elderly demographic [9].

### B. Diagnosis and Treatment

State-of-the-art approaches to manage (carotid) *atherosclerosis* exist on multiple levels. Asymptomatic patients can benefit from lifestyle changes and conservative treatments in order to reduce risk factors such as cigarette consumption or elevated blood and cholesterol levels. However, due to the effort associated with on-site monitoring techniques like electrocardiography, carotid (duplex) ultrasound, or even computed tomography angiography, only symptomatic patients are often recommended to undergo these procedures [10]. Structured screening is only conducted at a very low frequency since the stroke rates associated with asymptomatic carotid atherosclerosis are estimated at "only" around 1% per year [10]. It would be desirable to have low-effort high-frequency monitoring to address the remaining risk to the life of many patients with asymptomatic or undiagnosed carotid artery disease, as this could allow for more early-stage intervention and preemption of serious symptoms.

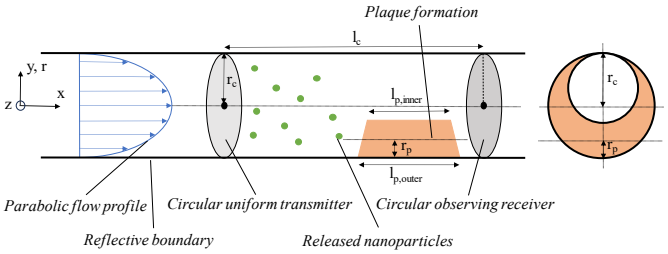


Fig. 1. Schematic diagram for the considered plaque scenario.The figure on the left shows the longitudinal section of the model, and the figure on the right shows the cross-section.

Once a stenosis becomes symptomatic or has reached a critical size, carotid artery disease treatments include surgical interventions like carotid endarterectomy and carotid artery stenting, aiming to restore adequate blood flow and reduce the risk of adverse cardiovascular events. Therefore, measures to react to carotid artery plaques are available, while at the same time, early-stage preventive diagnosis is not yet standard practice. Leveraging continuous communication inside the body as part of a future IoBNT could be a path towards monitoring and early detection of diseases, for example, *atherosclerosis*.

## III. Microfluidic MC Simulation

### A. Model Setup

In our three-dimensional (3D) scenario, we address the plaque formation in human carotids. The model follows Fig. 1. We assume a circular uniform transmitter and a circular observing receiver. The distance $l_c$ between transmitter and receiver, i.e., the length of the channel, is constant. We assume a constant distance of $l_c \in \{50, 100\}$ mm. For the radius of the channel representing the human carotid, $r_c$, we assume $r_c = 3.0\,\mathrm{mm}$, as the diameter $d_c$ is approximately equal to $6.0\,\mathrm{mm}$ [11]. Furthermore, we assume a flow with a mean velocity $v_{\mathrm{eff}} = 34.2\,\mathrm{cm/s}$, which is a good estimate for the blood flow velocity in common human carotid arteries [11]. Modeling the plaque formation, $r_p$ denotes the reduction in artery radius due to the plaque. In the following, we refer to $r_p$ relative to $r_c$. On the one hand, we consider the default case, which means that $r_p = 0 \times r_c$, i.e., the channel is a tube without any plaque formation. In addition, we consider the cases $r_p = 0.25 \times r_c$, $r_p = 0.5 \times r_c$, and $r_p = 0.75 \times r_c$. Parameters $l_{\mathrm{p,inner}}$ and $l_{\mathrm{p,outer}}$ denote the length of the plaque at the outside of the blood vessel and the length of the plaque inside the blood vessel, respectively. $l_{\mathrm{p,inner}} = 10.0\,\mathrm{mm}$ and

TABLE I
SIMULATION PARAMETERS

| Parameter | Value |
|---|---|
| Channel length $l_c$ [mm] | $\{50, 100\}$ |
| Radius $r_c$ [mm] | 3.0 |
| Mean velocity $v_{\text{eff}}$ [cm/s] | 34.2 |
| Radial expansion plaque $r_p$ | $\{0, 0.25, 0.5, 0.75\} \times r_c$ |
| Length plaque inside $l_{p,\text{inner}}$ [mm] | 10 |
| Length plaque outside $l_{p,\text{outer}}$ [mm] | 20 |

TABLE II
BOUNDARY CONDITIONS FOR THE VELOCITY AND THE PRESSURE.

| Boundary | Patch | Type | Value |
|---|---|---|---|
| Velocity [m/s] | inlet | *fixedValue* | $[0.342, 0, 0]$ |
| | outlet | *inletOutlet* | $[0, 0, 0]$ |
| | walls | *noSlip* | – |
| Kinematic pressure [$m^2/s^2$] | inlet | *fixedFluxPressure* | uniform 0 |
| | outlet | *fixedValue* | uniform 0 |
| | walls | *fixedFluxPressure* | uniform 0 |

$l_{\text{p,outer}} = 20.0\,\text{mm}$ are assumed to be constant. An overview of all simulation parameters can be found in Table I.

### B. Fluid, Particle, and Wall Parameters

#### 1) Fluid Properties

Targeting future use case families in the IoBNT, we consider human blood as a fluid for our simulations and assume a blood density of $1050\,\text{kg/m}^3$ [12]. Since blood is a non-Newtonian fluid, the ideal parabolic *Poiseuille* flow profile is not a valid model. The presence of larger objects, such as red blood cells, has been shown to result in a flattened front of the flow profile in practice. To capture this effect in our OpenFOAM simulation, the fluid's kinetic viscosity $\nu$ is expressed as a function of the shear stress rate $\dot{\gamma}$. In particular, we investigate and compare two models commonly used for blood in literature. Firstly, analogous to [13], we look at the non-Newtonian *Bird-Carreau* model of blood [14]. Here, blood's kinetic viscosity $\nu$ changes with respect to the fluid's rate of shear stress rate $\dot{\gamma}$ as

$$\nu = \nu_\infty + (\nu_0 - \nu_\infty)[1 + (k\dot{\gamma})^a]^{\frac{n-1}{a}}, \tag{1}$$

where $\nu_0$, $\nu_\infty$, $k$, and $n$ denote the kinematic viscosity of the fluid at zero shear rates, the kinematic viscosity of the fluid at an infinite shear rate, the relaxation time, and the power index, respectively. $a$ is a variable considering the change from linear behavior to power law. We assume the following parameters [13]: $\nu_0 = 3.3 \times 10^{-6}\,\text{m}^2/\text{s}$, $\nu_\infty = 1.32 \times 10^{-5}\,\text{m}^2/\text{s}$, $k = 0.6046\,\text{s}$, $n = 0.3742$, and $a = 2$.

We furthermore consider the *Casson* fluid model. It also characterizes the non-*Newtonian* behavior of a fluid and commonly serves as a basis model in blood rheology [15], specifying the lower ($\nu_{min}$) and upper ($\nu_{max}$) limits of viscosity. The model equation follows:

$$\nu = (\sqrt{\tau_0/\dot{\gamma}} + \sqrt{m})^2, \nu_{min} \leq \nu \leq \nu_{max}, \tag{2}$$

whereby $\dot{\gamma}$, $m$, and $\tau_0$ denote the fluid's shear stress rate, the *Casson* viscosity coefficient, and a threshold stress, respectively. We assume the following parameters for our fluid blood [16]: $m = 3.935 \times 10^{-6}\,\text{m/s}$, $\tau_0 = 2.9032 \times 10^{-6}\,\text{m/s}^2$, $\nu_{max} = 13.3333 \times 10^{-6}\,\text{m/s}$, and $\nu_{min} = 3.9047 \times 10^{-6}\,\text{m/s}$.

Unless otherwise specified, we will use the *Bird-Carreau* model in the following.

#### 2) Particle Properties

We assume superparamagnetic iron-oxide nanoparticles (SPIONs) as information carriers. SPIONs comprise an iron core accompanied by a biocompatible lauric acid coating to prevent clumping, typically possessing a hydrodynamic radius of 50 nm [17]. Due to their biocompatibility, SPIONs have found applications in various medical contexts, for example, in targeted drug delivery [18]. For the simulation study, we assume a fixed value size distribution. A total number of $n = 1000$ nanoparticles is released after the simulation has reached a quasi-stationary state. Following Fig. 2, the quasi-stationary state is achieved after approximately 0.3 s for both values of $l_c$. The start of injection (SOI), i.e., the release of the SPIONs, is defined as 0.4 s. The nanoparticles are released uniformly distributed over the entire cross-section of the circular uniform transmitter. We assume a density of $5175\,\text{kg/m}^3$ [19].

#### 3) Wall Properties

Analogous to [13], the walls are modeled as a rigid surface. Thereby, on the vessel wall, *noSlip* boundary conditions are applied. The *noSlip* boundary condition sets the patch velocity in all three spatial directions to zero, i.e., $\mathbf{v_{wall}} = [0\ 0\ 0]$.

### C. Boundary Conditions

At the inlet, the boundary condition for the velocity is specified as *fixedValue*. Consequently, the velocity at the inlet face is defined by the vector $[0.342\ 0\ 0]$ m/s across all three spatial directions, assuming a fluid flow velocity of $v_{\text{eff}} = 34.2\,\text{cm/s}$. For the walls, the boundary condition *noSlip* is applied, enforcing zero velocity at the patch in all three spatial directions. At the outlet, the *inletOutlet* boundary condition establishes the outflow of the system by imposing a zero gradient condition. This condition ensures that the field adopts the internal field value, maintaining continuity in the absence of a significant gradient at the outlet.

The pressure boundary condition at the inlet and at the walls is applied by the *fixedFluxPressure* condition. The *fixedFluxPressure* condition is employed in pressure scenarios, commonly incorporating the zero gradient condition. Conversely, the *fixedValue* condition is applied at the outlet. Table II provides an overview of the boundary conditions.

### D. Fluid Flow Parameters

All simulation cases are simulated assuming laminar flow — in this first measurement study, we neglect turbulence modeling. One can differentiate between laminar and turbulent flows by considering the ratio of the inertial forces to the viscous forces, known as the *Reynolds* number. The *Reynolds* number for flow in a pipe can be computed as [20]:

$$Re = \frac{v_{\text{eff}} \cdot D_H}{\nu}, \tag{3}$$

whereby $v_{\text{eff}}$, $D_H$ and $\nu$ denote the mean velocity in the tube, the hydraulic diameter of the tube (for a circular tube, the hydraulic diameter is equal to the diameter of the tube), and the kinematic viscosity. For $v_{\text{eff}} = 0.342\,\text{m/s}$, $D_H = 0.006\,\text{m}$, and $\nu = \{\nu_0, \nu_\infty\} = \{3.3{\times}10^{-6}, 1.32{\times}10^{-5}\}\text{m}^2/\text{s}$, it follows

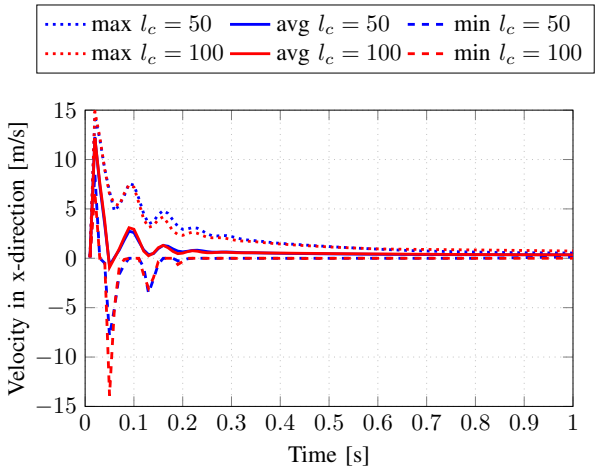


Fig. 2. Convergence to a steady state for various distances $l_c$ (in mm) conducted using the *simpleFoam* solver, excluding any interaction with injected particles. A quasi-stationary state is achieved in the two scenarios after approximately 0.3 s.

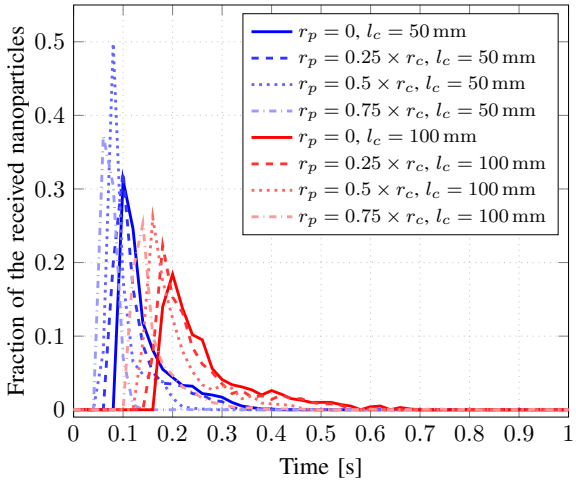


Fig. 4. Fraction of the received nanoparticles compared to the $n = 1000$ released nanoparticles for the two transmitter-receiver distances $l_c = 50\,\mathrm{mm}$, and $l_c = 100\,\mathrm{mm}$.

for the plain tube: $Re = \{621.82, 155.45\} < 2300$ [20], i.e., laminar flow regime. This is only a preliminary estimation for this initial study as turbulence modeling for non-Newtonian fluids and in a pipe with changing diameters is beyond the scope of this paper. Additionally, we note that the flow through the cardiovascular system, especially in large arteries near the heart, such as the carotid, exhibits a significant pulsed component. However, we assume that the propagation time frame of our study ($\approx 0.5\,\mathrm{s}$, see Fig. 4) is small compared to multiple pulse cycles of the heart, and we, therefore, neglect the pulsed component for this first study. Our assumption of constant flow would also be more generally valid in other blood vessels of smaller diameter or further from the heart [2].

In our simulation runs, we simulate a total time of 1.4 s, i.e., SOI plus 1 s simulation time of the released particles. The time interval $\Delta t$ for the simulation runs is constant, $\Delta t = 1 \times 10^{-4}\,\mathrm{s}$.

## IV. Results and Discussion

Fig. 4 shows the channel impulse response (CIR), i.e., the fraction of the received nanoparticles, for both transmitter-receiver distances, namely $l_c = 50\,\mathrm{mm}$ and $l_c = 100\,\mathrm{mm}$. In both scenarios, we see that the larger the radius of the plaque $r_p$, i.e., the smaller the narrowed cross-section of the channel, the sooner the released nanoparticles reach the receiver. For example, for $l_c = 100\,\mathrm{mm}$, the first nanoparticles arrive at the receiver 0.58 s after the SOI for the plain tube ($r_p = 0$), while for $r_p = 0.25 \times r_c$, $r_p = 0.5 \times r_c$, and $r_p = 0.75 \times r_c$ the first nanoparticles arrive 0.56 s, 0.54 s, and 0.52 s after the SOI, respectively. The faster arrival of the particles can be explained by the higher flow velocity in the narrowed channel caused by the Venturi effect [21], see Fig. 3. The plaque formation is accompanied by change in the flow velocity profile; see visual comparison of unaffected range 0–0.015 m and affected range 0.015–0.04 m in Fig. 3, where the velocity of the nanoparticles is significantly higher. Furthermore, it can be seen that the height of the peak increases up to $r_p = 0.5 \times r_c$, followed by a decrease which, however, gets smaller with increasing transmitter-receiver distance. An increase in channel length from 50 to 100 mm is associated with an added propagation delay of about 0.1 s and more particle dispersion over time.

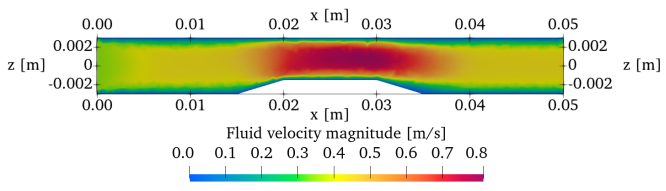


Fig. 3. Flow profile for the *Casson* model, for a plaque radius $r_p = 0.25 \times r_c$, and channel length $l_c = 50\,\mathrm{mm}$.

Fig. 5 depicts the cumulative CIR, i.e., the total number of received nanoparticles over time for the different values of $r_p$ and $l_c$. Analogous to Fig. 4, the faster arrival of the nanoparticles for larger plaques is represented by the earlier rise in the number of nanoparticles. Except for an added propagation delay, the channel length does not seem to impact the results significantly. Fig. 5 also depicts the asymptotic number of received nanoparticles, which appears to have reached a stable plateau in all cases at the end of the simulation. As expected, the plateau is reached faster for larger plaque sizes. Additionally and crucially, we also see a decrease in the asymptotic number of received nanoparticles for a growing plaque, i.e., some nanoparticles do not arrive at the receiver. While for $r_p \in \{0, 0.25\} \times r_c$, this fraction remains at 0%, for $r_p = 0.5 \times r_c$, approximately 5%, and for $r_p = 0.75 \times r_c$, around 25% of nanoparticles do not reach the receiver. An analysis of the 3D flow simulation results reveals that the plaque prevents some nanoparticles from moving on to the receiver, resulting in them not arriving or only arriving very slowly.

This effect on the asymptotic number of nanoparticles could be a crucial indicator of a growing plaque, as it is a marker that appears in the long-term consideration of the channel response and does not require precise timing or peak detection. It also explains the lowering of the peak for plaque radii greater than $0.5 \times r_c$ observed in Fig. 4 since the decrease in the total number of contributing nanoparticles will naturally also decrease the peak number of nanoparticles that pass through over time.

Finally, Fig. 6 shows a comparative analysis of the total number of received nanoparticles using the *Bird-Carreau* and the *Casson* fluid model. We can observe slight deviations between the two models but no fundamental difference in any

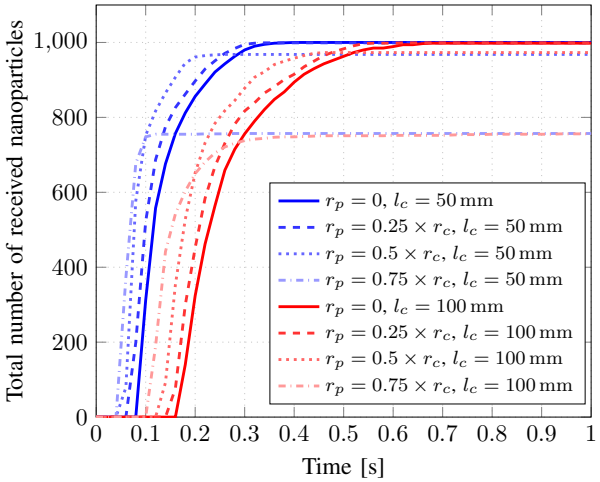


Fig. 5. Total number of the received nanoparticles for the two transmitter-receiver distances $l_c = 50\,\text{mm}$, and $l_c = 100\,\text{mm}$.

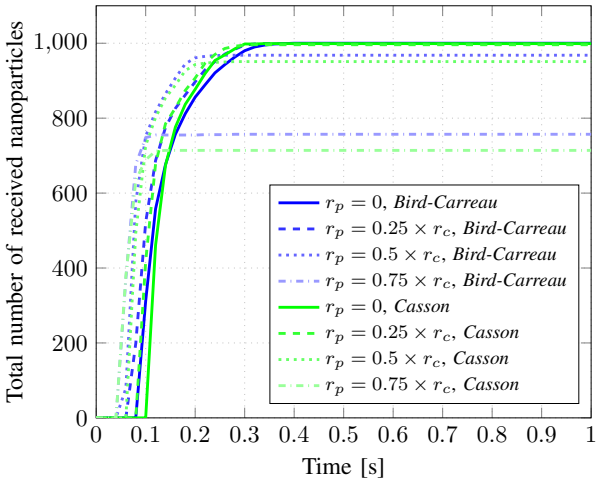


Fig. 6. Total number of received molecules under consideration of the *Bird-Carreau* versus the *Casson* model, as described in Section III-B for the transmitter-receiver distance $l_c = 50\,\text{mm}$.

of the previously outlined trends. This serves as a first sign of the consistency of the results under different assumptions, and we plan to expand our modeling scope further going forward.

## V. Conclusion and Future Research

In this paper, we have evaluated the effect of arterial plaque of different sizes on the CIR for a simplified MC link within a blood vessel. The results show that growing plaque is associated with a lower propagation delay and a reduction in the total number of received nanoparticles, as plaques with a radius $> 0.25 \times r_c$ prevent some nanoparticles from passing through the channel. It is important to note that this result, in particular, is dependent on our assumptions on the surface roughness resulting in stoppage of the particles, and a further investigation of more detailed models of arteries as MC channels is crucial for future work. However, increased surface roughness has previously been identified as a feature of sites of plaque growth, and they could, therefore, be associated with a higher likelihood of inhibiting some particles [22].

This is a preliminary step towards analyzing cardiovascular diseases from the perspective of communication theory in the context of the IoBNT vision, where BNM communicate inside the body. Future research will include more detailed arterial properties, such as blood vessel elasticity, and plaque formation scenarios. Investigating the complex effects of turbulence on propagation will also be an essential next step in capturing more detailed results.

## References

[1] I. F. Akyildiz, M. Pierobon, S. Balasubramaniam, and Y. Koucheryavy, "The Internet of Bio-Nano Things," *IEEE Commun. Mag.*, vol. 53, no. 3, Mar. 2015.

[2] L. Felicetti, M. Femminella, and G. Reali, "Simulation of Molecular Signaling in Blood Vessels: Software Design and Application to Atherogenesis," *Nano Communication Networks*, vol. 4, no. 3, pp. 98–119, Sep. 2013.

[3] L. Felicetti, M. Femminella, G. Reali, P. Gresele, M. Malvestiti, and J. N. Daigle, "Modeling CD40-Based Molecular Communications in Blood Vessels," *IEEE Transactions on NanoBioscience*, vol. 13, no. 3, pp. 230–243, Sep. 2014.

[4] V. Jamali, A. Ahmadzadeh, W. Wicke, A. Noel, and R. Schober, "Channel Modeling for Diffusive Molecular Communication—A Tutorial Review," *Proc. IEEE*, vol. 107, no. 7, Jun. 2019.

[5] I. Atthanayake, S. Esfahani, P. Denissenko, I. Guymer, P. J. Thomas, and W. Guo, "Experimental Molecular Communications in Obstacle Rich Fluids," in *Proc. 5th ACM Int. Conf. Nanoscale Comput. Commun.*, short paper, Reykjavik Iceland, Sep. 2018.

[6] A. S. Thalmayer, A. Ladebeck, S. Zeising, and G. Fischer, "Reducing Dispersion in Molecular Communications by Placing Decelerators in the Propagation Channel," *IEEE Trans. Mol. Biol. Multi-Scale Commun.*, Jul. 2023.

[7] R. Ross, "Atherosclerosis — An Inflammatory Disease," *New England Journal of Medicine*, vol. 340, no. 2, Jan. 1999.

[8] V. R. Preedy and R. R. Watson, Eds., *Handbook of Disease Burdens and Quality of Life Measures*. New York, NY: Springer, 2010.

[9] P. Song, Z. Fang, H. Wang, et al., "Global and Regional Prevalence, Burden, and Risk Factors for Carotid Atherosclerosis: A Systematic Review, Meta-Analysis, and Modelling Study," *The Lancet Global Health*, vol. 8, no. 5, May 2020.

[10] A. Thapar, I. H. Jenkins, A. Mehta, and A. H. Davies, "Diagnosis and Management of Carotid Atherosclerosis," *BMJ*, vol. 346, Mar. 2013.

[11] L. A. Ferrara, M. Mancini, R. Iannuzzi, et al., "Carotid Diameter and Blood Flow Velocities in Cerebral Circulation in Hypertensive Patients," *Stroke*, vol. 26, no. 3, Mar. 1995.

[12] T. Kenner, "The Measurement of Blood Density and its Meaning," *Basic Research in Cardiology*, vol. 84, no. 2, Mar. 1989.

[13] S. Yogeswaran and F. Liu, "Vascular Flow Simulations using SimVascular and OpenFOAM," *medRxiv*, Sep. 2021.

[14] Y. I. Cho and K. R. Kensey, "Effects of the Non-Newtonian Viscosity of Blood on Flows in a Diseased Arterial Vessel. Part 1: Steady Flows," *Biorheology*, vol. 28, no. 3-4, Jun. 1991.

[15] P. Decuzzi, F. Causa, M. Ferrari, and P. A. Netti, "The Effective Dispersion of Nanovectors Within the Tumor Microvasculature," *Annals of Biomedical Engineering*, vol. 34, no. 4, pp. 633–641, Apr. 2006. (visited on 04/19/2024).

[16] Chris Greenshields. "OpenFOAM v6 User Guide - 7.3 Transport/Rheology Models." (Jul. 2018), [Online]. Available: https://doc.cfd.direct/openfoam/user-guide-v6/transport-rheology (visited on 04/25/2024).

[17] M. Bartunik, J. Teller, G. Fischer, and J. Kirchner, "Channel Parameter Studies of a Molecular Communication Testbed with Biocompatible Information Carriers: Methods and Data," *IEEE Trans. Mol. Biol. Multi-Scale Commun.*, vol. 9, no. 4, Oct. 2023.

[18] R. Tietze, S. Lyer, S. Dürr, et al., "Efficient Drug-Delivery using Magnetic Nanoparticles — Biodistribution and Therapeutic Effects in Tumour Bearing Rabbits," *Nanomedicine: NBM*, vol. 9, no. 7, Oct. 2013.

[19] M. Kappes, B. Friedrich, F. Pfister, et al., "Superparamagnetic Iron Oxide Nanoparticles for Targeted Cell Seeding: Magnetic Patterning and Magnetic 3D Cell Culture," *Adv. Funct. Mater.*, vol. 32, no. 50, Aug. 2022.

[20] F. White, *Fluid Mechanics* (McGraw-Hill International Editions). WCB/McGraw-Hill, 1999.

[21] C. Schaschke, *A Dictionary of Chemical Engineering*. OUP Oxford, 2014.

[22] D. G. Owen, T. Schenkel, D. E. T. Shepherd, and D. M. Espino, "Assessment of Surface Roughness and Blood Rheology on Local Coronary Haemodynamics: A Multi-Scale Computational Fluid Dynamics Study," *J. R. Soc. Interface*, vol. 17, no. 169, Aug. 2020.

This article has been accepted for publication in IEEE Transactions on Molecular, Biological, and Multi-Scale Communications . This is the author's version which has not been fully edited content may change prior to final publication. Citation information: DOI 10.1109/TMBMC.2024.3423005



**Pit Hofmann** (Graduate Student Member, IEEE) received the Dipl.-Ing. degree from Technische Universität Dresden, Dresden, Germany, in 2021. He is currently pursuing a joint Ph.D. degree with the Deutsche Telekom Chair of Communication Networks, Faculty of Electrical and Computer Engineering, Technische Universität Dresden, and the Centre for Tactile Internet with Human-in-the-Loop (CeTI), Cluster of Excellence, Dresden, Germany. His research interests include molecular communications, biological computing, and nanonetworking.

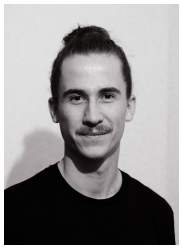

**Sebastian Schmidt** (Graduate Student Member, IEEE) received the B.Sc. and M.Sc. degrees in Electrical Engineering and Information Technology from the Technical University of Munich (TUM), Munich, Germany, in 2018 and 2022, respectively, with distinction. From 2023 to 2024, he was a graduate research assistant at the Chair of Communication Networks, TUM, where he worked on molecular communication networks and the Internet of Bio-Nano Things.

**Alexander Wietfeld** (Graduate Student Member, IEEE) received the B.Sc. and M.Sc. degrees in electrical engineering with a focus on communication engineering from RWTH Aachen, Aachen, Germany, with distinction in 2021 and 2023, respectively. He is currently pursuing the Dr.-Ing. degree at the Chair of Communication Networks, Technical University of Munich. His research interests are in the fields of molecular communication networks and the Internet of Bio-Nano Things, including work on multiple access techniques and resource optimization.


**Pengjie Zhou** received the B.S. in electronics and information engineering from Lingnan Normal University, Zhanjiang, China, in 2015 and the M.S. degree in analytic instruments, measurement- and sensor-technology from Hochschule Coburg, Coburg, Germany, in 2022. He is currently pursuing a Ph.D. degree with the Deutsche Telekom Chair of Communication Networks, Faculty of Electrical and Computer Engineering, Technische Universität Dresden, Dresden, Germany. His research interests include molecular communication, liquid-based experimental setups for molecular communications, and coding and modeling for diffusive molecular communications.

**Jonas Fuchtmann** received the master's degree in mechanical engineering with a focus on medical engineering from the Technical University of Munich (TUM), Munich, Germany, in 2018. He is currently pursuing a degree in medicine and is working as a researcher at the MITI Research Group of the University Hospital Rechts der Isar, Munich, Germany, since 2018. His research interests include technical assistive systems for surgical workflows and tele-medical applications.

**Frank H.P. Fitzek** (Senior Member, IEEE) received the Diploma (Dipl.-Ing.) degree in electrical engineering from the University of Technology Rheinisch-Westfälische Technische Hochschule, Aachen, Germany, in 1997, the Ph.D. (Dr.-Ing.) degree in electrical engineering from the Technical University Berlin, Germany, in 2002, and the Honorary degree (Doctor Honoris Causa) from the Budapest University of Technology and Economics, Budapest, Hungary, in 2015. He was an Adjunct Professor with the University of Ferrara, Italy, in 2002. In 2003, he joined Aalborg University as an Associate Professor, where he became a Professor. He co-founded several start-up companies, starting with acticom GmbH, Berlin, in 1999. He is currently a professor and the head of the Deutsche Telekom Chair of Communication Networks, Technische Universität Dresden, Germany, where he coordinates the 5G Lab Germany.

**Wolfgang Kellerer** (Senior Member, IEEE) is a Full Professor with the Technical University of Munich (TUM), Munich, Germany, heading the Chair of Communication Networks at the School of Computation, Information and Technology. He received his Ph.D. degree in Electrical Engineering from the same university in 2002. He was a visiting researcher at the Information Systems Laboratory of Stanford University, CA, US, in 2001. Prior to joining TUM, Wolfgang Kellerer pursued an industrial career, being for over ten years with NTT DOCOMO's European Research Laboratories. He was the director of the infrastructure research department, where he led various projects for wireless communication and mobile networking, contributing to research and standardization of LTE-A and 5G technologies. In 2015, he has been awarded with an ERC Consolidator Grant from the European Commission for his research on flexibility in communication networks. He currently serves as an associate editor for IEEE Transactions on Network and Service Management and as the area editor for network virtualization for IEEE Communications Surveys and Tutorials.